CD226⁻ Human Regulatory T Cells Exhibit Increased Stability Compared to Conventionally Sorted Populations

Matthew E. Brown[1], Juan M. Arnoletti[1], Lindsey K. Sachs[1], Kayla Q. Nguyen[1], Jin-Ju Lee[1] , Todd M. Brusko[1,2]

[1]Department of Pathology, Immunology and Laboratory Medicine, University of Florida, Gainesville, FL
[2]Department of Pediatrics, University of Florida, Gainesville, FL

Abstract

Previously, adoptive cell therapies (ACT) have sought to prevent autoimmunity in individuals with Type 1 Diabetes (T1D) using flow-activated cell sorting (FACS) and *in-vitro* expansion of CD4+CD25+CD127lo/- Tregs from peripheral blood. However, this methodology yields a heterogenous population of phenotypically stable, thymically derived FOXP3+/Helios+ (tTregs) and unstable, peripherally derived FOXP3+Helios- Tregs (pTregs). Here, we present a novel strategy for FACS isolation of Tregs with an increased proportion of tTregs using the profile CD4+CD25+CD226-. Flow cytometric assessment of canonical lineage-determining transcription factors demonstrated that isolation of CD226- Tregs yielded greater percentages of tTregs and reduced percentages of pTregs, both before (tTreg:+Δ4.70%, pTreg:-Δ1.10%) and after (+Δ3.57%, -Δ4.43%) a 14-day *in vitro* expansion, as compared to CD127- Tregs. Post-expansion, CD226- Tregs displayed an altered cytokine profile characterized by increased expression of extracellular (1.87-fold) and intracellular TGFb1 (1.15-fold) with decreased expression of IL-10 (0.83-fold), IFNg (0.86-fold), IL-17A (0.92-fold) and TNFa (0.79-fold), compared to CD127- Tregs. CD226- Tregs exhibited greater *in vitro* suppression than CD127- Tregs (+Δ22.0% at 1:1 Treg:PBMC ratio). CRISPR-Cas9 knockout (KO) of *CD226* supported the role of CD226 in lineage instability, with CD127- CD226 KO Tregs displaying higher tTreg (+Δ39.0%) and lower pTreg (-Δ13.9%) percentages compared to unedited CD127- Treg controls. These data suggests that CD226- Tregs are of increased phenotypic stability and possess a greater *in-vitro* suppressive capacity, having implications for ACT in the prevention or suspension of T1D.

CD226⁻ Tregs Demonstrate Increased Regulatory Function

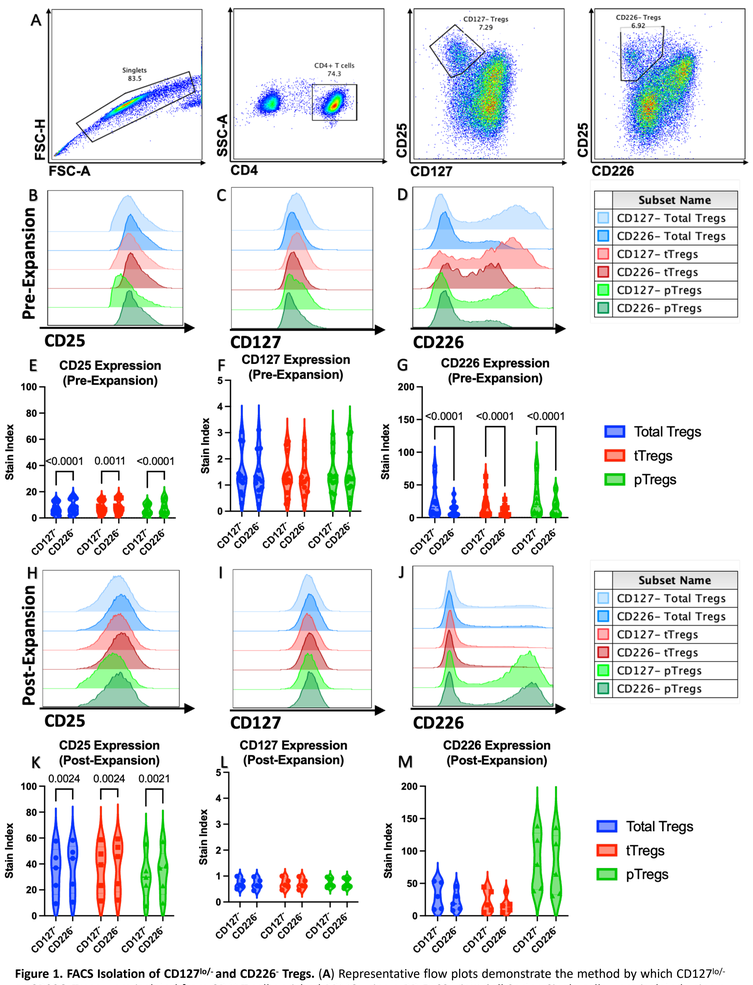

Figure 1. FACS Isolation of CD127$^{lo/-}$ and CD226⁻ Tregs. (**A**) Representative flow plots demonstrate the method by which CD127$^{lo/-}$ or CD226⁻ Tregs were isolated from CD4⁺ T-cell enriched PBMC using a BD FACSAriaIII Cell Sorter. Single cells were isolated using a forward scatter area (FSC-A) by forward scatter height (FSC-H) plot, followed by gating on CD4⁺ T cells. CD4⁺ T cells were then separated into CD25⁺CD127$^{lo/-}$ Tregs or CD25⁺CD226⁻ Tregs. Histograms show expression of (**B**) CD25, (**C**) CD127, and (**D**) CD226 for CD127$^{lo/-}$ (lighter blue) and CD226⁻ CD4⁺CD25⁺ FOXP3⁺ total Tregs (darker blue), CD127$^{lo/-}$ (lighter red) and CD226⁻ CD4⁺CD25⁺FOXP3⁺ Helios⁺ tTregs (darker red), and CD127$^{lo/-}$ (lighter green) and CD226⁻CD4⁺CD25⁺ FOXP3⁺Helios⁻ pTregs (darker green), prior to expansion. Fold changes of the stain index (SI) of (**E**) CD25, (**F**) CD226, and (**G**) TIGIT from either pre-expansion CD127$^{lo/-}$ sorted Treg or CD226⁻ sorted Treg cultures following gating on total Tregs, tTregs, and pTregs. Representative histograms show expression of (**H**) CD25, (**I**) CD127, and (**J**) CD226 for CD127$^{lo/-}$ (lighter blue) and CD226⁻ (darker blue) total Tregs, CD127$^{lo/-}$ (lighter red) and CD226⁻ (darker red) tTregs, and CD127$^{lo/-}$ (lighter green) and CD226⁻ (darker green) pTregs, following 14 days of *in vitro* expansion. Fold changes of the SI of (**K**) CD25, (**L**) CD127, and (**M**) CD226 from either 14-day *in vitro* expanded CD127$^{lo/-}$ sorted Treg or CD226⁻ sorted Treg cultures following gating on total Tregs, tTregs, and pTregs.

CD226⁻ Treg Isolation Yields Higher Proportions of Stable Thymic Tregs

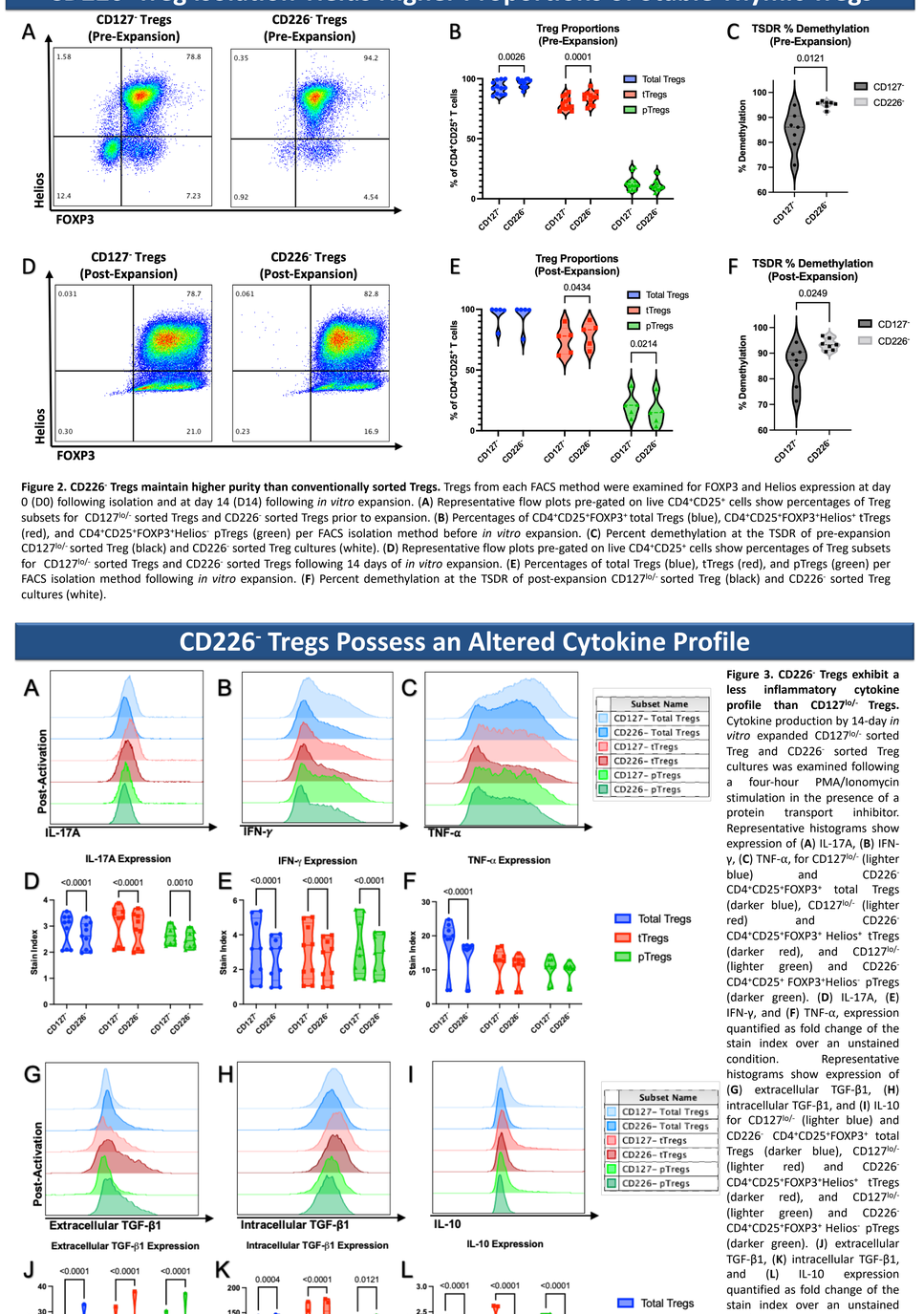

Figure 2. CD226⁻ Tregs maintain higher purity than conventionally sorted Tregs. Tregs from each FACS method were examined for FOXP3 and Helios expression at day 0 (D0) following isolation and at day 14 (D14) following *in vitro* expansion. (**A**) Representative flow plots pre-gated on live CD4⁺CD25⁺ cells show percentages of Treg subsets for CD127$^{lo/-}$ sorted Tregs and CD226⁻ sorted Tregs prior to expansion. (**B**) Percentages of CD4⁺CD25⁺FOXP3⁺ total Tregs (blue), CD4⁺CD25⁺FOXP3⁺Helios⁺ tTregs (red), and CD4⁺CD25⁺FOXP3⁺Helios⁻ pTregs (green) per FACS isolation method before *in vitro* expansion. (**C**) Percent demethylation at the TSDR of pre-expansion CD127$^{lo/-}$ sorted Treg (black) and CD226⁻ sorted Treg cultures (white). (**D**) Representative flow plots pre-gated on live CD4⁺CD25⁺ cells show percentages of Treg subsets for CD127$^{lo/-}$ sorted Tregs and CD226⁻ sorted Tregs following 14 days of *in vitro* expansion. (**E**) Percentages of total Tregs (blue), tTregs (red), and pTregs (green) per FACS isolation method following *in vitro* expansion. (**F**) Percent demethylation at the TSDR of post-expansion CD127$^{lo/-}$ sorted Treg (black) and CD226⁻ sorted Treg cultures (white).

CD226⁻ Tregs Possess an Altered Cytokine Profile

Figure 3. CD226⁻ Tregs exhibit a less inflammatory cytokine profile than CD127$^{lo/-}$ Tregs. Cytokine production by 14-day *in vitro* expanded CD127$^{lo/-}$ sorted Treg and CD226⁻ sorted Treg cultures was examined following a four-hour PMA/Ionomycin stimulation in the presence of a protein transport inhibitor. Representative histograms show expression of (**A**) IL-17A, (**B**) IFN-γ, (**C**) TNF-α, for CD127$^{lo/-}$ (lighter blue) and CD226⁻ CD4⁺CD25⁺FOXP3⁺ total Tregs (darker blue), CD127$^{lo/-}$ (lighter red) and CD226⁻ CD4⁺CD25⁺FOXP3⁺ Helios⁺ tTregs (darker red), and CD127$^{lo/-}$ (lighter green) and CD226⁻ CD4⁺CD25⁺ FOXP3⁺Helios⁻ pTregs (darker green). (**D**) IL-17A, (**E**) IFN-γ, and (**F**) TNF-α, expression quantified as fold change of the stain index over an unstained condition. Representative histograms show expression of (**G**) extracellular TGF-β1, (**H**) intracellular TGF-β1, and (**I**) IL-10 for CD127$^{lo/-}$ (lighter blue) and CD226⁻ CD4⁺CD25⁺FOXP3⁺ total Tregs (darker blue), CD127$^{lo/-}$ (lighter red) and CD226⁻ CD4⁺CD25⁺FOXP3⁺Helios⁺ tTregs (darker red), and CD127$^{lo/-}$ (lighter green) and CD226⁻ CD4⁺CD25⁺FOXP3⁺ Helios⁻ pTregs (darker green). (**J**) extracellular TGF-β1, (**K**) intracellular TGF-β1, and (**L**) IL-10 expression quantified as fold change of the stain index over an unstained condition.

CD226⁻ Tregs Are More Naïve

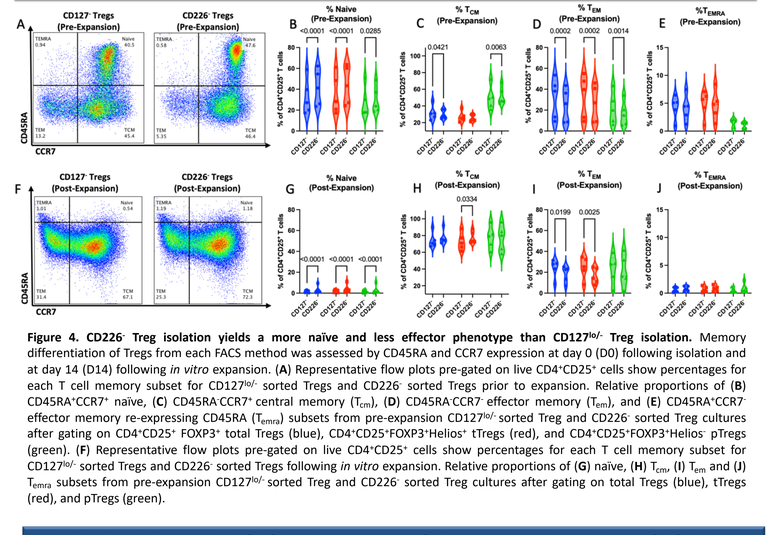

Figure 4. CD226⁻ Treg isolation yields a more naïve and less effector phenotype than CD127$^{lo/-}$ Treg isolation. Memory differentiation of Tregs from each FACS method was assessed by CD45RA and CCR7 expression at day 0 (D0) following isolation and at day 14 (D14) following *in vitro* expansion. (**A**) Representative flow plots pre-gated on live CD4⁺CD25⁺ cells show percentages for each T cell memory subset for CD127$^{lo/-}$ sorted Tregs and CD226⁻ sorted Tregs prior to expansion. Relative proportions of (**B**) CD45RA⁺CCR7⁺ naïve, (**C**) CD45RA⁻CCR7⁺ central memory (T_{cm}), and (**D**) CD45RA⁻CCR7⁻ effector memory re-expressing CD45RA (T_{emra}) subsets from pre-expansion CD127$^{lo/-}$ sorted Treg and CD226⁻ sorted Treg cultures after gating on CD4⁺CD25⁺ FOXP3⁺ total Tregs (blue), CD4⁺CD25⁺FOXP3⁺Helios⁺ tTregs (red), and CD4⁺CD25⁺FOXP3⁺Helios⁻ pTregs (green). (**F**) Representative flow plots pre-gated on live CD4⁺CD25⁺ cells show percentages for each T cell memory subset for CD127$^{lo/-}$ sorted Tregs and CD226⁻ sorted Tregs following *in vitro* expansion. Relative proportions of (**G**) naïve, (**H**) T_{cm}, (**I**) T_{em} and (**J**) T_{emra} subsets from pre-expansion CD127$^{lo/-}$ sorted Treg and CD226⁻ sorted Treg cultures after gating on total Tregs (blue), tTregs (red), and pTregs (green).

CD226⁻ Tregs Exhibit Increased Suppressive Capabilities

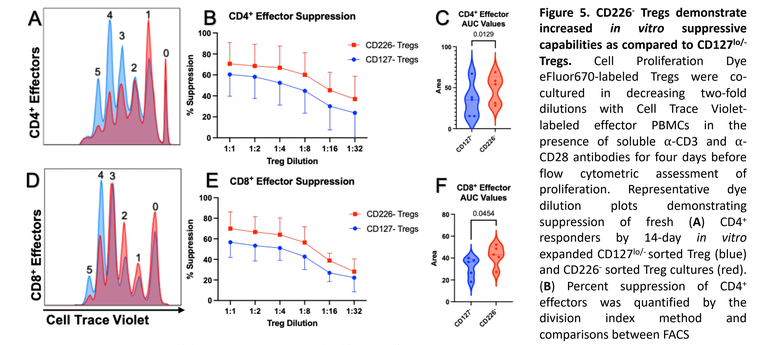

Figure 5. CD226⁻ Tregs demonstrate increased *in vitro* suppressive capabilities as compared to CD127$^{lo/-}$ Tregs. Cell Proliferation Dye eFluor670-labeled Tregs were co-cultured in decreasing two-fold dilutions with Cell Trace Violet-labeled effector PBMCs in the presence of soluble α-CD3 and α-CD28 antibodies for four days before flow cytometric assessment of proliferation. Representative dye dilution plots demonstrating suppression of fresh (**A**) CD4⁺ responders by 14-day *in vitro* expanded CD127$^{lo/-}$ sorted Treg (blue) and CD226⁻ sorted Treg cultures (red). (**B**) Percent suppression of CD4⁺ effectors was quantified by the division index method and comparisons between FACS conditions were made using (**C**) area under the curve (AUC) values for each percent suppression curve. Representative dye dilution plots demonstrating suppression of fresh (**D**) CD8⁺ responders by 14-day *in vitro* expanded CD127$^{lo/-}$ sorted Treg (blue) and CD226⁻ sorted Treg cultures (red). (**E**) Percent suppression of CD4⁺ effectors was quantified by the division index method and comparisons between FACS conditions were made using (**F**) area under the curve (AUC) values for each percent suppression curve.

Conclusions

The results of this study suggest that CD226⁻ Treg isolation yields a **higher percentage of tTregs**, which augments the lineage stability of the isolated population. Furthermore, these CD226⁻ Tregs demonstrated increased therapeutic potential for adoptive cell therapy applications, with a **reduced inflammatory profile** and **increased suppressive capabilities**, *ex vivo,* compared to conventionally sorted CD127- Tregs. These findings highlight the importance of further research into the role of CD226 and Treg instability as well as evaluating the potential of CD226 as a therapeutic target for Tregs to inhibit the pathogenesis of Type 1 Diabetes.

Future Directions

- **CRISPR Cas9** gene-editing to knockout (KO) *CD226* in human Tregs
  - Assess Treg lineage stability without CD226 co-stimulation
- **α-CD226 Activating mAbs** co-culture with sorted human Tregs
  - Associate CD226 costimulation with decreased Treg stability
- **α-CD226 Blocking mAbs** for transient blockade of CD226 on Tregs in the NOD Mouse Model
  - Potential for increased Treg stability, resulting in reduced disease incidence
- **CAR-Treg** development to generate tissue-specific CD226⁻ Tregs
  - Identify whether CD226 reductions increase therapeutic efficacy of CAR-Tregs

Project support was provided by grants from the National Institutes of Health (R01 DK106191 to TMB; HIRN UG3 DK122638 to TMB)